Assessing the turbulence in a tidal estuary and the effect of turbulence on marine current turbine performance

Maxime Thiébaut, Alexei Sentchev, François G Schmitt

Assessing tidal turbine performance and the relationship between the turbine output power and turbulence in a tidal estuary

Alexei Sentchev*[1], Maxime Thiébaut*[2], François G. Schmitt†[3]
*Laboratoire d'Océanologie et de Géosciences (UMR 8187),
Université du Littoral - Côte d'Opale, 32 avenue Foch, 62930 Wimereux, France.
[1]alexei.sentchev@univ-littoral.fr
[2]maxime.thiebaut@univ-littoral.fr
†Laboratoire d'Océanologie et de Géosciences (UMR 8187),
CNRS, 28 avenue Foch, 62930 Wimereux, France.
[3]françois.schmitt@cnrs.fr

***Abstract*—A series of tidal turbine tests were conducted in a tidal estuary (the Sea Scheldt, Belgium) as a part of activities of the European project Pro-Tide (Interreg IVB NW Europe). Two prototypes of in-stream vertical axis tidal turbine were tested in real conditions during several weeks in winter 2014 and late summer 2015. Tidal current velocity variations were continuously recorded by a downward looking Acoustic Doppler Current Profiler (ADCP), operating at 1 Hz and two Acoustic Doppler Velocimeters (ADV) operating at 16 and 32 Hz. The measurements covered different tidal current regimes: strong flood and ebb flow with velocity above 1.2 m/s and also a flow reversal. Turbulence intensity in the surface layer and its variations with time and with depth were estimated. Scaling properties of the turbulent flow such as dissipation rate (ϵ), integral scale (L), and Kolmogorov scale (η) were also quantified. Using the output power generated by a Darrieus type turbine and the tidal flow velocity time series, the turbine performance was estimated and the impact of turbulence on power production was quantified. The results show that, in high frequency band, fluctuations of the output power are driven by turbulence in the tidal flow. The coherence spectrum shows tight correlations in both high (inertial) and low frequency bands. The overall performance of the turbine was assessed by evaluating the power coefficient, C_p. A low variation of C_p around the mean value of 0.25 was observed for a large range of flow velocities.**

***Index Terms*—Tidal turbine testing - Turbulence - Power coefficient - Tidal estuary**

I. Introduction

In recent years, full-scale prototypes of tidal-stream turbines have been used as pre-commercial demonstrators in many countries. Advancements in hydrokinetic power conversion from tidal currents require detailed understanding of the fluid velocities surrounding devices, in particular the turbulence. Experience in the wind energy industry indicates that turbulence is the primary cause of fatigue and thus determines the life expectancy of a turbine. However, assessment of turbulent properties of a powerful tidal flow in natural conditions is arduous exercise. For this reason, analysis of a possible link between "local turbulence strength" and energy conversion device performance are generally performed using a theoretical framework of energy multifractal cascades [1], experimental approach (in a flume tank) [2], [3] and modelling approach [4], [5].

Mycek et al. [6] studied the wake induced by a single three bladed turbine in a flume tank. They showed that the wake generated by turbine is widely influenced by the ambient turbulence rate. The authors also documented a reduction in power coefficient by roughly 10% caused by the ambient turbulence intensity increase from 3% to 15%. This range of turbulence level variation is considered in experimental studies [7], [8].

A number of in situ surveys performed at tidal energy sites revealed a turbulent intensity rate ranging from 8 to 11% for tidal current velocities of the order of 1.5-2 m/s [9]–[12].

In this paper, the results of in-stream tidal turbine tests, conducted in a tidal estuary (the Sea Scheldt, Belgium) as a part of activities of the European project Pro-Tide (Interreg IVB NW Europe) are presented. Using the tidal flow velocity time series recorded simultaneously with the output power generated by turbines, the major turbulent properties of the tidal flow are estimated and the performance of tidal turbines is evaluated. Turbulent properties of the flow are assessed for different flow conditions covering periods with turbine test runs and natural tidal flow regime. This enables to quantify the change in turbulence level caused by the running turbine which can be further used in numerical simulations.

II. Data and methods

A. Experimental site and settings

The experimental site, located westward of Antwerp, was designed to receive in-stream Darrieus type turbines for testing in real conditions during a period of several months. The flow regime in the estuary is strongly dominated by tides of semi-diurnal period. The tidal range is of the order of 6 m with a slight fortnight modulation. Tidal current velocities attain the maximum values of 1.5 m/s and 1.9 m/s during neap and spring tide respectively. A typical cycle of tidal flow evolution

is shown in Fig. 2. Flood tide lasts approximately 7 hours and ebb tide 5.5 hours. The slack water duration is very short and the tidal current velocity changes from 1 m/s to -1 m/s in 0.5 hour, after the current reversal (CR) of low water (LW). The mean ebb flow velocity is 0.2 m/s higher than the mean flood flow velocity. This difference is caused by a particular shape of the velocity curve with a pronounced saddle point at flood flow (Fig. 2).

A floating pontoon (3 m x 39 m) was installed in the middle of the Sea Scheldt between two piles oriented in the streamwise direction. At pontoon location, the river width and mean depth are approximately 300 m and 8 m. Tidal turbines were installed at a side of the pontoon. Current velocities were recorded simultaneously by ADV and ADCP, both installed on a steel rail at the extremity of the pontoon downstream the turbine. ADV was aligned with the middle line of the turbine whereas ADCP was out of line by approximately 1 m.

B. ADV data

Acoustic Doppler Velocimeters (ADV of Nortek) was recording 3 components of the flow velocity at 16 Hz, 1 m below the surface. The measurements covered different tidal current regimes: strong ebb and flood flow with velocity above 1.2 m/s and also a flow reversal (Fig. 2). A total of four deployments were performed at test site using identical configuration. During one deployment, two ADV recorded simultaneously velocities with sampling frequency set to 16 and to 32 Hz. The longest period of data acquisition lasted 12 tidal cycles (11.09 – 18.09 2015). The distance between the tidal turbine and ADV is estimated as $12D$ (18 m) with D being the turbine diameter (Fig. 1). The recorded horizontal velocities were projected on along- and cross-shore axes of the river flow by rotating the tidal current ellipse clockwise by 23^o. Time series of the streamwise velocity (u component) and cross-flow velocity (v component) were thus generated for further analysis. The quality of the ADV data was very good and data filtering appeared not necessary.

C. ADCP data

A 1.2-MHz downward-looking four-beam broadband RDI ADCP, mounted on a fixed frame next to ADV, recorded current velocity during different periods of turbine test runs. The instrument was operated in fast pinging mode 12, providing one instantaneous velocity profile per second. Each velocity record was an average of three short pulse measurements over a second interval providing the accuracy of velocity acquisition of 0.04 m/s. Velocities were recorded in beam coordinates with 0.25 m vertical resolution (bin size), starting from 0.9 m below the surface (midpoint of the first bin). In this study, the velocity data provided by ADCP were used for tidal flow characterisation, comparison with ADV data and evaluation of the kinetic power available in the flow.

D. Vertical Axis Hydro Turbines

Two Darrieus type Vertical Axis Hydro Turbines (VAHT) of "Water2Energy" company (Netherlands) and "Blue Energy Canada" company were tested during six week period each in winter 2014 and late summer 2015 respectively. The dimensions of the two turbines are the following: 1.5 m high (H) and 2 m diameter (D) for the first turbine and 1 m high and 1.5 m diameter for the second turbine. Both devices are four blade, pitch controlled turbines, with a capability to produce power during the entire tidal cycle including ebb and flood flow, and a cut-in-speed of 0.5 m/s. Output power of each turbine was recorded at 100 Hz acquisition frequency.

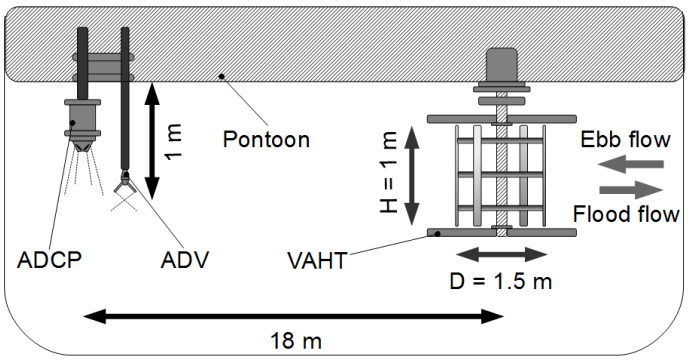

Fig. 1. Schematic side view of the experimental setup. The ADV was installed at a distance of 12 times the diameter D.

E. Methods of flow characterization, turbulent properties and output power assessment

The assessment of the major properties of tidal flow is done using the current velocity time series provided by ADV and ADCP. The time averaged (1-min interval), overall mean velocity magnitude, and maximum velocity are estimated. Current asymmetry and turbulence properties of the flow are also quantified.

Tidal flow asymmetry, representing the difference between the velocity magnitude on flood and ebb flow, can cause a considerable imbalance of power production during a tidal cycle. The following expression was used to estimate the tidal current asymmetry a:

$$a = \frac{< u_{flood} >}{< u_{ebb} >} \tag{1}$$

where brackets mean time averaging of the velocity magnitude on flood and ebb tide.

The ambient turbulence level is another metric conventionally used in tidal energy projects. This quantity provides insight into both the extreme and fatigue loads that would be applied to an in-stream turbine. The streamwise turbulence intensity is defined as:

$$I_u = \frac{\sigma_u}{< u >} \tag{2}$$

where σ_u and $U =< u >$ denote the standard deviation and the mean of the streamwise velocity magnitude respectively. The averaging is performed over 2-hour periods of maximum current speed on ebb and flood tide.

The value of the dissipation rate ϵ is estimated using the power spectrum of the velocity time series assuming Kolmogorov relationship of the local isotropic turbulence [13]:

$$E(k) = C\epsilon^{2/3}k^{-5/3} \quad (3)$$

where C is a constant ($C \simeq 1.5$) and k the wavenumber. Frequency and wavenumber are related with the velocity magnitude u averaged over analyzed period such as: $k = 2\pi f/U$. Thus, the dissipation rate can be estimated from the power spectrum as [14], [15]:

$$\epsilon = (\frac{C_0}{C})^{3/2}(\frac{2\pi}{U})^{5/2} \quad (4)$$

where C_0 is a constant such as $E(f) = C_0 f^{-5/3}$ is the best fit estimated over the inertial range.

The value of ϵ allows to determine two other flow scaling properties: an integral scale L (largest injection length scale) and the Kolmogorov dissipation scale η defined by:

$$L = \frac{\sigma_u^3}{\epsilon} \quad (5)$$

and

$$\eta = (\frac{\nu^3}{\epsilon})^{1/4} \quad (6)$$

where σ_u is the standard deviation of the streamwise velocity and ν, the kinematic viscosity of water ($\nu = 1.5\ 10^{-6} m^2/s$).

III. Results

A. Tidal dynamics in the estuary and turbulent properties of the flow

Tidal flow in the Sea Scheldt is predominantly alternative: the magnitude of streamwise velocity component is ten times higher than that of cross-flow component. The current velocity vector draws an ellipse of low eccentricity (Fig. 3). Tidal current ellipse reveals a light misalignment between flood and ebb flow (direction asymmetry) of the order of 7^o, in the surface layer. Moreover, the current velocity asymmetry varies from 0.7 to 0.75 during different velocity surveys. The mean ebb flow velocity exceeded 1 m/s whereas the mean flood flow velocity was close to 0.8 m/s. In addition, flood tide lasts 1.5 h longer than ebb tide (Fig. 2). The highest velocity values are reached immediately after the LW on ebb tide and at HW on flood tide.

A very low range of variation of the cross-flow velocity component v, compared to streamwise component u (Fig. 4), allows to justify the choice of turbulent intensity I_u used in analysis. The magnitude of high frequency fluctuations for both velocity components is similar and ranges within 0.03 m/s for $u < 1$ m/s and within 0.05 m/s for $u > 1$m/s on flood tide (Fig. 4b). On ebb tide, the range of variations is slightly higher (σ_u = 0.07 m/s, σ_v = 0.06 m/s). Significantly small mean values of cross-flow velocity increase artificially the turbulence intensity estimate if a combination of horizontal velocity components is used. For this reason, in further analysis of turbulence and comparison with output power production, only the streamwise velocity time series u are used. Table I provides the turbulent intensity values I_u estimated for flood and ebb tide periods with velocity exceeding 0.5 m/s. Turbulent intensity derived from ADCP appears slightly lower on flood than on ebb flow (9.5 and 11.0 %). However these values are found overestimated by 20-30% when compared to respective quantities derived from ADV (6.5 and 8.5 %). Such a difference was already documented in previous studies [14]. The running turbine increases the level of turbulence in the wake, behind the turbine. ADV measurements revealed a large

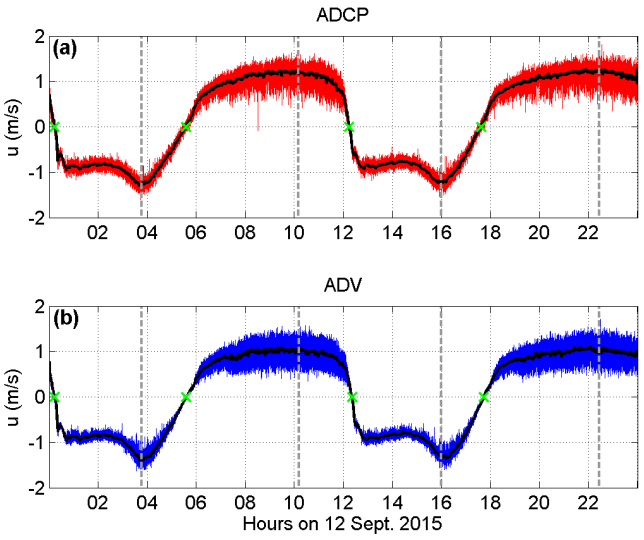

Fig. 2. Time series of the streamwise velocity u measured by ADCP (a) and ADV (b) on 12 September 2015. Grey dashed lines show peak velocity values recorded during ebb flow (u positive) and flood flow(u negative). Zero velocity values are shown by green crosses.

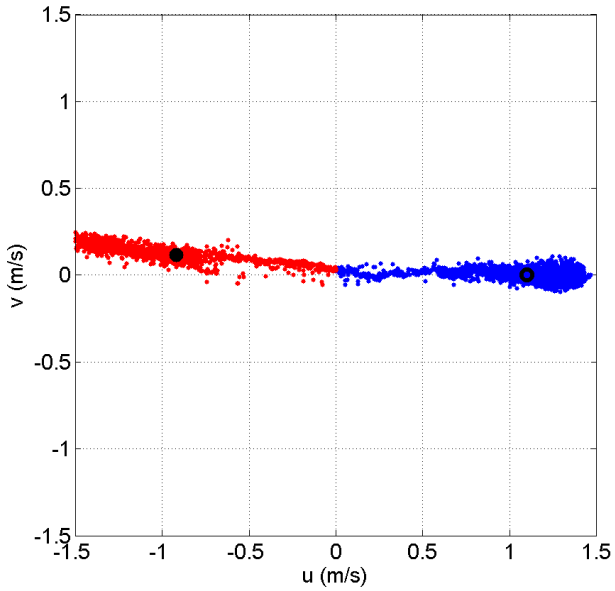

Fig. 3. Tidal current ellipse derived from ADV measurements. Red and blue points represent velocity of flood and ebb flow respectively. Full and empty circles indicate the time average flood and ebb flow velocity values.

TABLE I
TURBULENT INTENSITY ESTIMATED 1 M BELOW THE SURFACE

	Without turbine		With turbine	
Tidal stage	Flood	Ebb	Flood	Ebb
ADV	6.5	8.5	7.5	16.0
ADCP	9.5	11.0	10.0	13.0

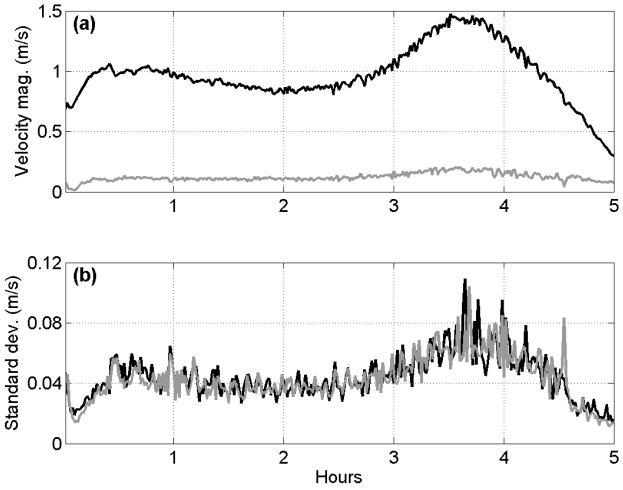

Fig. 4. (a) Velocity magnitude (1-min averaged) of the streamwise component (black) and cross-flow component (grey). (b) Standard deviation of velocity components estimated during flood flow prior to turbine deployment.

difference (nearly 100%) compared to the level of turbulence in the free flow. However, the ADCP velocity records reveal only 10 to 20% increase of I_u (Table I). This can be related to lower frequency (1 Hz) and to spatial averaging of velocity recording by ADCP.

Velocity variations (Fig. 2) clearly show a different level of ambient turbulence between ebb and flood flow, with and without turbine runs, which can be also quantified through spectral analysis of velocity time series. Fig. 5 shows the power spectral density (PSD) of velocity recorded by ADV during two successive periods of a tidal cycle on September 8, 2015. Only periods with average velocity exceeding 0.5 m/s were used in calculations. This enables further comparison with spectral analysis of the output power generated by tidal turbine.

Regarding the velocity variations, three frequency ranges can be identified in Fig. 5: inertial range, limited by 10^{-1} Hz and 4 Hz, high frequency range ($f > 4$ Hz) with PSD curve changing the slope due to noise in the data, and low frequency range ($f < 10^{-1}$ Hz). In the inertial range, the spectral slope is -5/3, suggesting that the energy of large scale eddies is cascading in this frequency band.

In the low frequency range, the spectral slope is close to -1/2, the hypothesis of homogeneous and isotropic turbulence is not respected, and the analysis of velocity fluctuations can not be performed in the framework of Kolmogorov's theory.

Three fundamental properties of the turbulent flow are estimated using the PSD distribution in the inertial range: the dissipation rate ε, integral scale L, and Kolmogorov scale η. The two latter parameters are related with characteristic size of motions in tidal current in the estuary: size of eddies generated in (homogeneously) turbulent flow and the smallest scale at which the fluid is affected by viscosity.

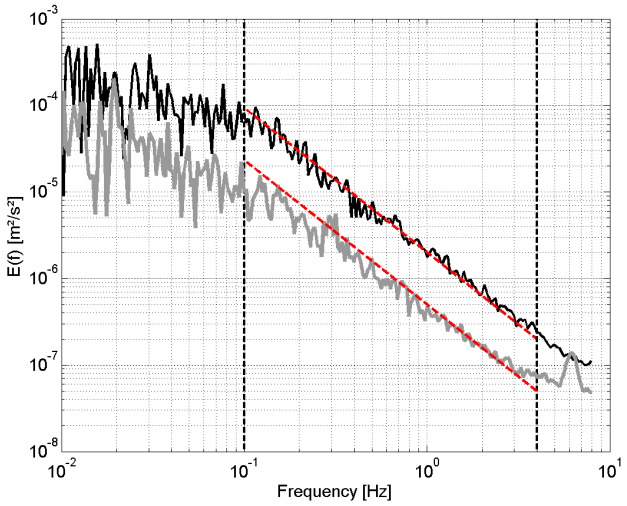

Fig. 5. Power specral density of streamwise velocity with (black) and without (grey) turbine running. Black dashed lines delimit the range where the classic $f^{-5/3}$ slope is observed (red dashed lines).

Turbulent properties of the ebb flow derived from ADV data are compared for two particular conditions: with and without running turbine. ADV data collected prior to turbine deployment and during the turbine test runs were analysed. Scaling parameters of the turbulent flow are summarized in Table II. The magnitude of the dissipation rate is 25 times higher downstream of the running turbine than in a (non disturbed) tidal flow. This means that much more turbulent kinetic energy is transformed into thermal energy when the turbine was running. The value of ϵ which is found in both cases is very high corresponding to the level which is commonly found in a surface layer of coastal water flow. A characteristic size of turbulent eddies (integral scale L) in the free flow is close to 2 m. The running turbine blades destroy these eddies and reduce the integral scale of energy injection by a factor of 2.

Finally, the Kolmogorov scale is found lower in the turbulent wake produced by the turbine than in the non disturbed flow. It reveals that the turbulence causes a light decrease of dissipation scale η at which a viscous molecular diffusion of energy takes place.

B. Joint analysis of power production and flow variability

PSD of the output power generated by Water2Energy turbine (Fig. 6) reveals the -5/3 spectral slope for a larger frequency range (from 10^{-2} Hz to 2 Hz). Even if two high peaks in PSD distribution are found at frequencies f_0 (rotor working frequency) and $4f_0$ (frequency at which four blades

TABLE II
TURBULENT FLOW ESTIMATION

Scaling flow properties	$\epsilon(m^2s^{-3})$	$L(m)$	$\eta(mm)$
Without turbine	$2\ 10^{-4}$	1.7	0.3
With turbine	$5\ 10^{-3}$	0.8	0.2

interacts with the flow), the shape of the spectrum and its slope suggest that the output power is strongly affected by turbulence. Fig. 5 and Fig. 6 show that fluctuations of power in the range $10^{-2} - 2$ Hz have properties identical to that of the turbulent tidal flow.

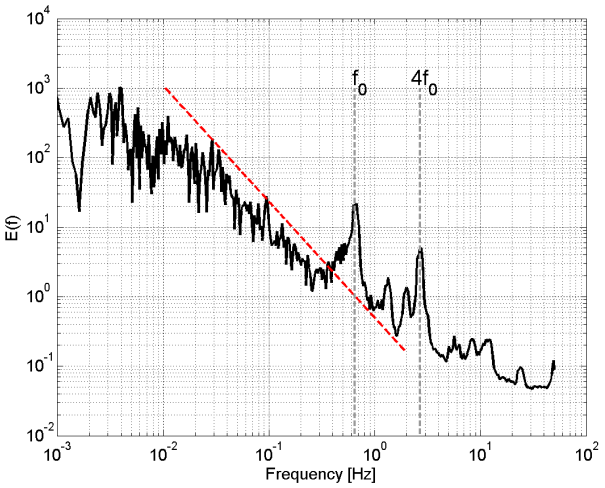

Fig. 6. Spectrum of output power genrerated by Dutch Water2Energy turbine. Red dashed line shows the -5/3 slope in the inertial range.

To further assess this effect, the coherency spectrum γ_{xy} was estimated as the Fourrier transform of the covariance function of two time series: flow velocity and output power. The coherency spectrum represents the ratio of the modulus of the co-spectrum E_{xy} by the square root of the product of both spectra [16]:

$$\gamma_{xy} = \frac{|E_{xy}(f)|}{[E_{xx}(f)E_{yy}(f)]^{1/2}} \tag{7}$$

γ_{xy} varies from 1 to less than 0.7 (Fig. 7) indicating the degree of correlation between x(velocity) and y (power). In low frequency range, the power production is completely determined by the flow velocity ($P \sim U^3$). In the frequency range from $5\ 10^{-4}$ Hz to $3\ 10^{-2}$ Hz, the correlation varies showing rather noisy behaviour. In the range from 0.1-0.2 Hz to 2 Hz (inertial range) the correlation is stable thus indicating that the output power fluctuations are caused to major extent by the turbulence in tidal flow [8].

C. Power coefficient

The efficiency of Dutch Water2Energy tidal turbine was evaluated by estimating the power coefficient C_p for a number of turbine runs generating the power at flood flow. Fig. 8c

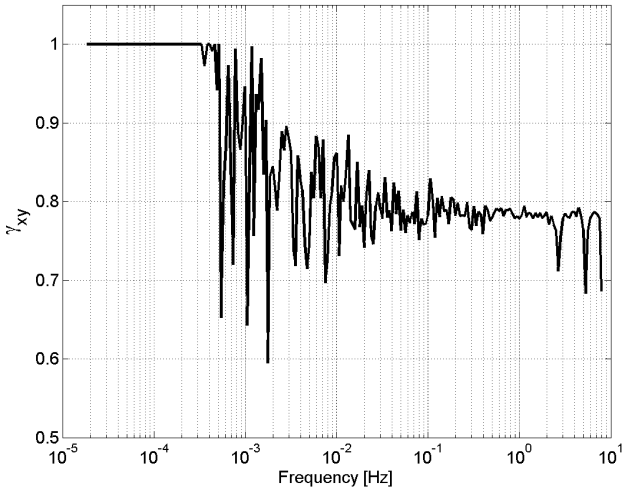

Fig. 7. Coherency spectrum between flow velocity and output power.

shows an example of the output power produced by the turbine on 8 November, 2014 and tidal current velocities recorded by ADCP. Both data sets were 1-min averaged (black lines in Fig. 8a and 8b). Peak power production (1200 W) is reached for a peak velocity of 1.25 m/s. For the same period, Fig. 8c shows the power P generated by the turbine versus the maximum available power P_∞ of the flow incoming through the turbine rotor. Two subsets are identified: $P_\infty \in$ [300; 2000] W and $P_\infty \in$ [2300; 3000] W. Both sets are separated by a jump of output power occuring for current speed rising from 1.1 m/s to 1.15 m/s (P_∞ = 2000 W and P_∞ = 2300 W respectively). Since output power is related to velocity cubed, even modest increases in speed can lead to significant gain in power production. For each subsets, the power coefficient C_p is estimated from the linear fit. Results provides C_p of 0.25 and 0.24 for $P_\infty <$ 2000 W and $P_\infty >$ 2300 W respectively. For the first interval, the confidence in C_p estimation is really high. 95% of experimental points (output power and available power) lie within $\pm$ 2 std range (std = 17 W/m^2), evidencing a low spreading. The correlation is also very high (R = 0.98). For the second interval, spreading is slightly bigger (std = 57 W/m^2) and correlation drops to 0.72. Analysis of the output power and velocity records for other dates of the turbine test period provided similar results.

IV. CONCLUSIONS

Two prototypes of in-stream vertical axis tidal turbine were deployed in the Sea Sheldt. Tidal velocity measurements were performed by ADCP and ADV during the turbine runs and natural tidal flow. Turbulent properties were estimated under both configurations (with and without turbine runs) and compared to assess the effect of turbulence on marine current turbine performance. Results reveal that the running turbine increases the background level of turbulence. Turbulent intensity (I_u) derived from ADCP show values overestimated by 25% on average in comparison to I_u provided by ADV.

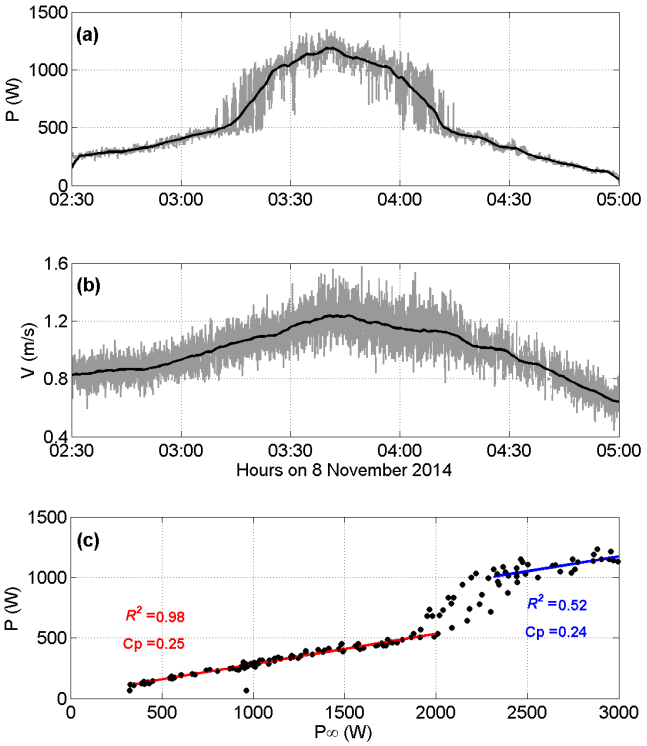

Fig. 8. Output power recorded during 2.5-hour long period on 8 November 2014 (a) and corresponding tidal current velocities provided by ADCP (b). Raw data are plotted in grey and 1-min averaged power and velocities in black. Comparison of the output power and the available kinetic power of the flow (1-min averaged) is presented in (c). Linear regression (red and blue lines) is used to estimate C_p for two subsets of data.

The dissipation rate ϵ was estimated through Fourier spectra in the frequency range where the classic $f^{-5/3}$ was observed it was estimated to be 25 times bigger downstream of the running turbine than in the non disturbed tidal flow. From ϵ values, the integral scale L and Kolmogorov scale η were quantified. It was demonstrated that the running turbine blades destroy the turbulent eddies of the free flow by reducing L by a factor of 2. Estimates of Kolmogorov scale revealed lower values in the wake than in the undisturbed flow (0.2 and 0.3 mm respectively).

Coherency spectrum between flow velocity and output power generated by the Water2Energy turbine was performed. Results show a tight correlation in both high and low frequency bands separated by a large interval with correlation strongly affected by noise.

Finally, the performance of the Dutch turbine was evaluated by quantifying the power coefficient C_p. It was estimated to be 0.25 on average.

ACKNOWLEDGMENTS

The authors would like to acknowledge the support of the Interreg IVB (NW Europe) "Pro-Tide" Program. The authors also ackowledge Reiner Rijke (Water2Energy) and Jon Ellison (Blue Energy Canada) for supplying the output power data recorded during tidal turbines testing and Roeland Notele for offering technical support during the fieldwork surveys. The skill and experience of Eric Lecuyer and his help during the fieldwork are appreciated and acknowledged.

REFERENCES

[1] U. Frish, *The legacy of A.N. Kolmogorov*. Cambridge University Press, 1995.

[2] T. Blackmore, L. E. Myers, and A. S. Bahaj, "Effects of turbulence on tidal turbines: Implications to performance, blade loads, and condition monitoring," *International Journal of Marine Energy*, vol. 14, pp. 1–26, 2016.

[3] I. A. Milne, A. H. Day, R. N. Sharma, and R. G. J. Flay, "The characterisation of the hydrodynamic loads on tidal turbines due to turbulence," *Renewable and Sustainable Energy Reviews*, vol. 56, pp. 851–864, 2016.

[4] W. M. J. Batten, A. S. Bahaj, A. F. Molland, and J. R. Chaplin, "The prediction of the hydrodynamic performance of marine current turbines," *Renewable energy*, vol. 33, no. 5, pp. 1085–1096, 2008.

[5] G. Pinon, P. Mycek, G. Germain, and E. Rivoalen, "Numerical simulation of the wake of marine current turbines with a particle method," *Renewable Energy*, vol. 46, pp. 111–126, 2012. [Online]. Available: http://www.sciencedirect.com/science/article/pii/S0960148112002418

[6] P. Mycek, B. Gaurier, G. Germain, G. Pinon, and E. Rivoalen, "Experimental study of the turbulence intensity effects on marine current turbines behaviour. Part II: Two interacting turbines," *Renewable Energy*, vol. 68, pp. 876–892, 2014.

[7] ——, "Experimental study of the turbulence intensity effects on marine current turbines behaviour. Part I: One single turbine," *Renewable Energy*, vol. 66, pp. 729–746, 2014.

[8] O. D. Medina, F. G. Schmitt, R. Calif, G. Germain, and B. Gaurier, "Turbulence analysis and multiscale correlations between synchronized flow velocity and marine turbine power production," *Renewable Energy (submitted)*, 2016.

[9] E. Osalusi, J. Side, and R. Harris, "Structure of turbulent flow in EMEC's tidal energy test site," *International Communications in Heat and Mass Transfer*, vol. 36, no. 5, pp. 422–431, 2009.

[10] J. Thomson, B. Polagye, M. Richmond, and V. Durgesh, "Quantifying turbulence for tidal power applications," in *OCEANS 2010*. IEEE, 2010, pp. 1–8.

[11] I. A. Milne, R. N. Sharma, R. G. J. Flay, and S. Bickerton, "Characteristics of the turbulence in the flow at a tidal stream power site," *Philosophical Transactions of the Royal Society of London A: Mathematical, Physical and Engineering Sciences*, vol. 371, no. 1985, p. 20120196, Feb. 2013.

[12] J. MacEnri, M. Reed, and T. Thiringer, "Influence of tidal parameters on SeaGen flicker performance," *Philosophical Transactions of the Royal Society of London A: Mathematical, Physical and Engineering Sciences*, vol. 371, no. 1985, p. 20120247, 2013.

[13] S. B. Pope, *Turbulent flows*. IOP Publishing, 2001.

[14] J. Thomson, B. Polagye, V. Durgesh, and M. C. Richmond, "Measurements of turbulence at two tidal energy sites in Puget Sound, WA," *Oceanic Engineering, IEEE Journal of Oceanic Enginnering*, vol. 37, no. 3, pp. 363–374, 2012.

[15] P. R. Renosh, F. G. Schmitt, H. Loisel, A. Sentchev, and X. Mériaux, "High frequency variability of particle size distribution and its dependency on turbulence over the sea bottom during re-suspension processes," *Continental Shelf Research*, vol. 77, pp. 51–60, 2014.

[16] J. S. Bendat and A. G. Piersol, *Random data: analysis and measurement procedures*. John Wiley & Sons, 2011, vol. 729.